

cell regeneration observed in adult recovery from bone-marrow aplasia that is mainly composed of memory CD4<sup>+</sup> T cells (18). The trend toward normalization of CD4<sup>+</sup> T cells displaying the CD28 costimulatory molecule (8) observed in our studies reflects the lower CD4<sup>+</sup> T cell activation and might allow for some recovery from enhanced sensitivity to apoptosis or anergy (19). The loss of memory CD4<sup>+</sup> T cell reactivity to recall antigens was indeed reversible under efficient antiviral therapy. This latter observation contrasts with the limited benefit for CD4<sup>+</sup> T cell function reported with zidovudine alone, where a weaker reduction in viral load (-1 log) could only increase preexisting CD4<sup>+</sup> T cell responses but failed to restore a lost T cell reactivity to recall antigens (20). The significant but partial restoration of CD4<sup>+</sup> T cell proliferation to recall antigens that we report might participate to the progressive regeneration of mature peripheral CD4<sup>+</sup> T cells observed after the first month of treatment, in agreement with murine models (21, 22).

This sequence of events suggests that, in the natural course of a productive infection, HIV activity per se is the driving force for chronic immune stimulation; the latter would take part in the defects in antigen-specific CD4<sup>+</sup> T cell activation and proliferation noted in HIV-infected patients (6, 7). Because such functions are required for a normal homeostasis of mature peripheral T cells in adults (21), their alteration would appear as a key mechanism in HIV-induced CD4<sup>+</sup> T cell depletion. This impairment of the mature CD4<sup>+</sup> cell repopulation process was, in part, reversible under effective antiviral treatment, although the balance between CD4<sup>+</sup> and CD8<sup>+</sup> subsets was not yet normalized with CD8<sup>+</sup> counts still higher than normal and CD4<sup>+</sup> counts remaining below normal thresholds. Earlier or stronger therapeutic interventions should reasonably achieve better reversibility.

## REFERENCES AND NOTES

1. M. Markowitz *et al.*, *N. Engl. J. Med.* **333**, 1534 (1995); R. Gulick *et al.*, in *Third National Conference on Human Retroviruses and Related Diseases*, Washington, DC, 28 January to 1 February 1996; A. C. Collier *et al.*, *N. Engl. J. Med.* **334**, 1011 (1996); D. Mathez *et al.*, *Antiretroviral Ther.*, in press.
2. W. Wei *et al.*, *Nature* **373**, 117 (1995); D. D. Ho *et al.*, *ibid.*, p. 123.
3. D. E. Mosier *et al.*, *ibid.* **375**, 193 (1995).
4. R. B. Effros *et al.*, *AIDS* **10**, F17 (1996); K. C. Wolthers *et al.*, *Science* **274**, 1543 (1996).
5. M. Roederer *et al.*, *J. Clin. Invest.* **95**, 2061 (1995).
6. J. V. Giorgi, *Immunology of HIV Infection* (Plenum, New York, 1996), p. 181.
7. H. C. Lane *et al.*, *N. Engl. J. Med.* **313**, 79 (1985); J. V. Giorgi *et al.*, *J. Immunol.* **138**, 3725 (1987); M. Clerici *et al.*, *J. Clin. Invest.* **82**, 1908 (1988).
8. B. Autran *et al.*, data not shown.
9. M. Merkleklager *et al.*, *Eur. J. Immunol.* **18**, 1653 (1988).
10. T. F. Tedder *et al.*, *J. Immunol.* **134**, 2989 (1985).
11. S. S. Kansas, *Blood* **88**, 3259 (1996).
12. S. M. Schnittman *et al.*, *Proc. Natl. Acad. Sci. U.S.A.* **87**, 6058 (1990).
13. T. Hara *et al.*, *J. Exp. Med.* **164**, 1988 (1986).
14. M. Levaucher *et al.*, *Clin. Exp. Immunol.* **90**, 376 (1992); J. V. Giorgi *et al.*, *J. Acquired Immune Defic. Syndr.* **6**, 904 (1993); M. Boffill *et al.*, *AIDS* **10**, 827 (1996).
15. J. Sprent, *Curr. Opin. Immunol.* **5**, 433 (1993); D. F. Tough *et al.*, *Immunol. Rev.* **150**, 129 (1996).
16. C. Aussel *et al.*, *Cell. Immunol.* **155**, 436 (1994).
17. W. Cavert *et al.*, *Science* **276**, 960 (1997).
18. C. L. Mackall *et al.*, *N. Engl. J. Med.* **332**, 143 (1995).
19. N. J. Borthwick *et al.*, *AIDS* **8**, 431 (1994).
20. A. D. Kelleher *et al.*, *J. Infect. Dis.* **173**, 321 (1996).
21. B. Rocha and H. von Boehmer, *Science* **251**, 1225 (1991).
22. C. Tanchot and B. Rocha, *Eur. J. Immunol.* **25**, 2127 (1995).
23. D. Mathez *et al.*, *Antimicrob. Agents Chemother.* **37**, 2206 (1993).
24. B. Autran *et al.*, *J. Immunol.* **154**, 1408 (1995).
25. We thank the clinicians participating in the therapeutic trial: A. G. Saimot, I. Gorin, G. Pialoux, and P. De Truchis; V. Calvez for analyzing HIV-1 plasma viral load; J. P. Chauvin from Abbott Laboratories for sponsoring the clinical trial; D. Faudot and M. Hirn from Coulter/Immunotech for kindly providing reagents; and SIDACTION and the Agence Nationale de Recherches sur le SIDA for financial support.

12 February 1997; accepted 7 May 1997

## Chemical Coupling Between Atmospheric Ozone and Particulate Matter

Z. Meng, D. Dabdub, J. H. Seinfeld\*

A major fraction of ambient particulate matter arises from atmospheric gas-to-particle conversion. Attempts to reduce particulate matter levels require control of the same organic and nitrogen oxide (NO<sub>x</sub>) emissions that are precursors to urban and regional ozone formation. Modeling of the gas-aerosol chemical interactions that govern levels of particulate components showed that control of gas-phase organic and NO<sub>x</sub> precursors does not lead to proportionate reductions of the gas-phase-derived components of atmospheric particles. The chemical coupling between ozone and particulate matter has implications for strategies to achieve the new ozone and particulate matter standards proposed by the U.S. Environmental Protection Agency.

Ozone has historically been regarded as the principal urban and regional air quality problem in the United States (1). Epidemiological evidence that urban mortality rates are correlated with mass concentration of fine particulate matter has now focused intense interest on reducing levels of airborne particles (2). In November 1996, the U.S. Environmental Protection Agency (EPA) proposed new ozone (O<sub>3</sub>) and particulate matter air quality standards (3). Because exposure to lower O<sub>3</sub> concentrations over longer periods of time than the current standard (0.12 parts per million averaged over a 1-hour period) is deemed to be of primary relevance, EPA proposed to lower the O<sub>3</sub> standard to 0.08 ppm averaged over an 8-hour period. EPA also proposed to revise the existing particulate matter (PM) standard to add two new PM<sub>2.5</sub> (particulate matter of diameter less than or equal to 2.5 μm) standards set at 15

μg m<sup>-3</sup> for the annual mean, and 50 μg m<sup>-3</sup> over a 24-hour period. Hundreds of counties in the United States in addition to those already in violation of the current standards are estimated to violate either or both of the new O<sub>3</sub> and PM standards (4).

Ozone and PM have traditionally been considered as separate problems. However, O<sub>3</sub> and PM are chemically coupled, and this coupling is of profound importance in understanding processes that control the levels of both. Urban and regional ozone abatement strategies have, for more than a decade, been evaluated with three-dimensional atmospheric models by the EPA and state and local agencies (1). We report here the application of a three-dimensional, size- and chemically resolved gas-aerosol model to examine how the chemical coupling that exists between O<sub>3</sub> and PM influences joint control of the two classes of pollutants.

The common components of atmospheric particles, such as sulfate (SO<sub>4</sub><sup>2-</sup>), nitrate (NO<sub>3</sub><sup>-</sup>), ammonium (NH<sub>4</sub><sup>+</sup>), organic compounds, crustal material, and water, reach the particulate phase by several different processes (Fig. 1). Aside from the direct emission of particles into the atmosphere, gas-to-particle conversion processes play an essential role in determining the mass of airborne PM. Such processes depend intimately on the organic

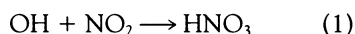
Z. Meng, Department of Environmental Engineering Science, California Institute of Technology, Pasadena, CA 91125, USA.

D. Dabdub, Department of Mechanical and Aerospace Engineering, University of California, Irvine, CA 92717-3975, USA.

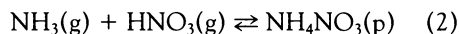
J. H. Seinfeld, Department of Chemical Engineering and Division of Engineering and Applied Science, California Institute of Technology, Pasadena, CA 91125, USA.

\*To whom correspondence should be addressed. E-mail: john\_seinfeld@starbase1.caltech.edu

and  $\text{NO}_x$  gas-phase chemistry that generates ozone (Fig. 2). Gas-phase organic and  $\text{NO}_x$  chemistry is driven by the hydroxyl (OH) radical, the levels of which depend on the mixture of organics and the organic/ $\text{NO}_x$  relative concentrations (5). Gas-phase conversion of  $\text{SO}_2$  to aerosol sulfate occurs by means of the reaction  $\text{SO}_2 + \text{OH}$ , which leads to  $\text{H}_2\text{SO}_4$  vapor molecules that rapidly transfer to the particulate phase by nucleation or condensation on existing aerosol surfaces (6, 7). In the presence of fogs or clouds, aqueous-phase conversion of  $\text{SO}_2$  to sulfate takes place, for example, by dissolved hydrogen peroxide ( $\text{H}_2\text{O}_2$ ) or  $\text{O}_3$  (8), and  $\text{H}_2\text{O}_2$  concentrations depend indirectly on the OH concentration. Hydrogen peroxide is itself a gas-phase product of the  $\text{HO}_2\text{-HO}_2$  reaction. A dominant termination reaction in the photochemical  $\text{O}_3$  system is the production of nitric acid



As the most ubiquitous basic gas in the atmosphere, ammonia provides a route for the formation of particulate-phase nitrate by means of the reversible reaction (9)



where (g) denotes gas phase and (p) denotes particulate phase. Secondary organic aerosol results when a parent organic molecule A reacts with OH,  $\text{O}_3$ , or  $\text{NO}_3$  to yield semivolatile products that partition themselves between the gas and aerosol phases (10).

The major gas-phase sinks of  $\text{NO}_x$  are  $\text{HNO}_3$  and peroxyacetyl nitrate (PAN),  $\text{CH}_3\text{C}(\text{O})\text{OONO}_2$ . Because of its reversible formation through reaction of peroxyacetyl radicals  $\text{CH}_3\text{C}(\text{O})\text{OO}\cdot$  (sometimes denoted  $\text{RCO}_3$ ) and  $\text{NO}_2$ ,



PAN serves as a temporary  $\text{NO}_x$  reservoir. Once formed,  $\text{HNO}_3$  may either be removed by deposition or, in the presence of  $\text{NH}_3$ , form particulate  $\text{NH}_4\text{NO}_3$ . Gas-phase photochemistry determines the relative amounts of  $\text{HNO}_3$  and PAN formed, and the amount of  $\text{NH}_3$  present governs the subsequent split between  $\text{HNO}_3$  loss by deposition and particulate  $\text{NH}_4\text{NO}_3$  formation.

Gas-phase  $\text{HNO}_3$  has a relatively high affinity to deposit on virtually any surface, a process termed dry deposition. A layer of  $\text{HNO}_3$  uniformly distributed up to a height of 1 km has a half-life as a result of dry deposition of about 30 hours (11). Particulate  $\text{NH}_4\text{NO}_3$ , on the other hand, has an affinity for dry deposition that is about an order of magnitude less than that of  $\text{HNO}_3$

(12). Consequently, for a layer of  $\text{NH}_4\text{NO}_3$  particles uniformly distributed up to a height of 1 km, the half-life is an order of magnitude larger than that of  $\text{HNO}_3$  vapor. In its role in converting  $\text{HNO}_3$  to  $\text{NH}_4\text{NO}_3$ , ammonia therefore exerts a direct influence on the airborne lifetime of nitrate. At low  $\text{NH}_3$  concentrations, more of the nitrate remains in the gas phase as  $\text{HNO}_3$ , where it is subject to dry deposition. In contrast, at higher concentrations of  $\text{NH}_3$ , more of the total nitrate is converted to particulate  $\text{NH}_4\text{NO}_3$ , and because of the lower dry deposition rate of particles, the overall atmospheric lifetime of nitrate is

increased. As  $\text{HNO}_3$  is removed by dry deposition, the  $\text{HNO}_3/\text{NH}_3/\text{NH}_4\text{NO}_3$  equilibrium can be shifted back toward the gas phase, causing  $\text{NH}_4\text{NO}_3$  to evaporate. Converting  $\text{NH}_4\text{NO}_3$  back into  $\text{HNO}_3$ , which is subject to an enhanced rate of dry deposition, serves to shorten the overall atmospheric lifetime of oxidized nitrogen.

Three-dimensional urban and regional ozone models have been in existence for two decades (13). We report here on the application of a three-dimensional Eulerian urban and regional atmospheric model designed to study the dynamics of trace gases and aerosols (14). Gas-to-particle conver-

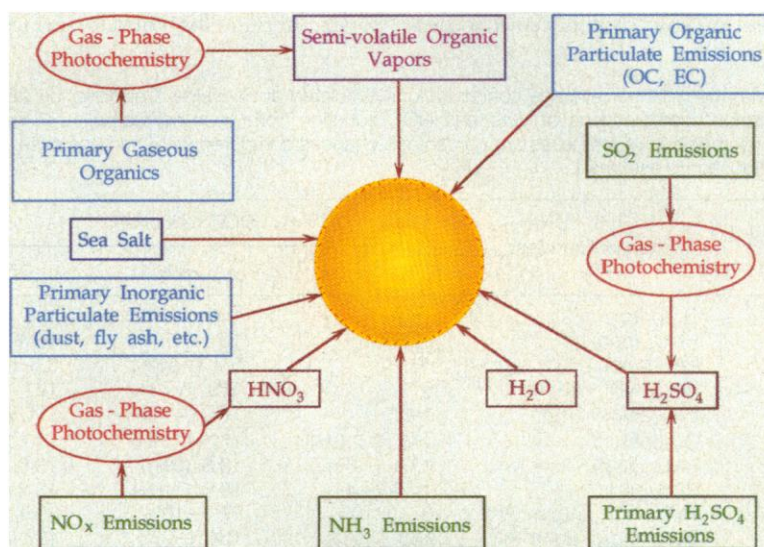
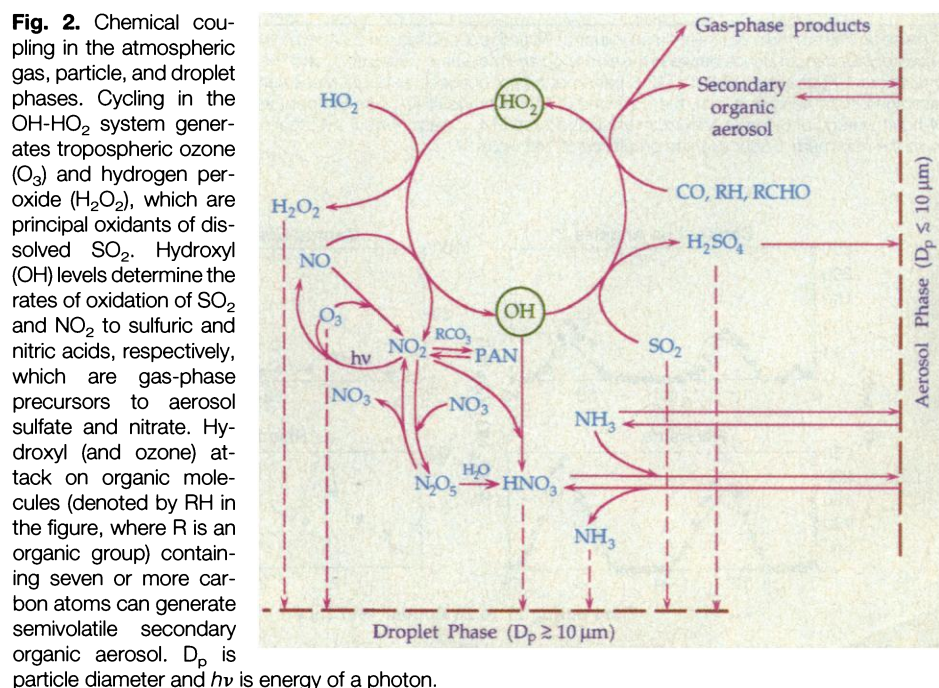


**Fig. 1.** Routes of incorporation of chemical species into atmospheric particulate matter. OC and EC denote organic and elemental carbon; other species are defined in the text.



sion is represented by dynamic mass transfer between the gas and aerosol phases. The model uses an  $80 \times 30$  rectangular master grid in the  $x, y$  plane. The computational domain corresponds to an irregular region within this grid composed of 994 columns of cells. Each column corresponds to a 5-km by 5-km region in the  $x, y$  plane and extends 1100 m in height. The columns are partitioned into five cells in the  $z$  direction. Each cell contains 40 gas-phase chemical species and 17 aerosol-phase species distributed over particle-size sections, between 0.04 and 10  $\mu\text{m}$  in diameter.

Ambient particles generally consist of a mixture of volatile and nonvolatile components. Soil material is nonvolatile; elemental and organic carbonaceous species

emitted directly from sources are also assumed to be nonvolatile. In the atmosphere the molecular transfer of volatile species such as  $\text{HNO}_3$ ,  $\text{NH}_3$ ,  $\text{H}_2\text{O}$ , and secondary organics between the gas and particulate phases tends to drive the overall gas-aerosol distribution of volatile species toward thermodynamic equilibrium. Water establishes equilibrium virtually instantaneously as compared with the characteristic time scale over which the aerosol is evolving, but theory shows that volatile inorganic species such as  $\text{NH}_4\text{NO}_3$  may or may not achieve equilibrium rapidly, depending on the prevailing temperature, relative humidity, and aerosol surface area (9). Treatment of this approach to equilibrium for volatile species is an

essential component of the gas-aerosol model (15).

The South Coast Air Basin of California (metropolitan Los Angeles), in spite of considerable improvements in air quality over the last two decades, continues to exhibit the most severe ozone and particulate matter air quality problem in the United States. For this reason, and because this region has the world's most extensive gas and particulate matter database against which to evaluate the performance of atmospheric models, we examined the chemical coupling between ozone and PM control in that area. We performed an extensive test of the performance of the model in simulating available data on gases and aerosols in the South Coast Air Basin from 27 to 28 August 1987, a period during the Southern California Air Quality Study (SCAQS) that experienced exceedingly high ozone and PM levels and for which a comprehensive gas-aerosol database exists (16).

Performance of the model in simulating the 27 to 28 August 1987 episode was analyzed by Meng *et al.* (17). Figure 3 shows the observed and predicted levels of  $\text{O}_3$  and  $\text{PM}_{2.5} \text{NO}_3^-$  at the Central Los Angeles and Riverside monitoring stations. A question critical to model application is the degree of uncertainty in predictions as a result of uncertainties in model inputs. It is well established that the most uncertain input in Los Angeles air pollution modeling is the volatile organic compound (VOC) inventory (18). Varying the total area-wide VOC emissions by  $\pm 25\%$  produces little change in  $\text{PM}_{2.5}$  levels, so input uncertainties do not appear to affect the use of the model to explore the phenomenology of joint control of ozone and PM.

The sensitivity of PM levels to emission reductions of organics and  $\text{NO}_x$  can be assessed by systematically changing source emissions by prescribed factors. We considered a matrix of control strategy cases (Table 1). Entries in the table indicate maxi-

**Table 1.** Maximum 1-hour average concentrations simulated at Riverside, California, on 28 August 1987 for various combinations of VOC and  $\text{NO}_x$  reduction from base estimated 1987 basinwide emissions. Numbers in parentheses are percentage changes compared with the base case. No  $\text{NH}_3$  emission reduction is assumed.

$\text{NO}_x$ reduction	Chemical species	VOC reduction		
		0%	25%	50%
0%	$\text{O}_3$ (ppb)	180*	146 (-19%)	119 (-34%)
	$\text{HNO}_3$ (ppb)	13.8*	16 (+17%)	16 (+17%)
	PAN (ppb)	13.7*	5.7 (-58%)	3.3 (-76%)
	$\text{PM}_{2.5} \text{NO}_3^-$ ( $\mu\text{g m}^{-3}$ )	97*	119 (+23%)	121 (+25%)
	$\text{PM}_{2.5}$ mass ( $\mu\text{g m}^{-3}$ )	146*	173 (+18%)	175 (+19%)
25%	$\text{O}_3$ (ppb)	175 (-2.6%)	172 (-4%)	170 (-6%)
	$\text{HNO}_3$ (ppb)	13.4 (-3%)	13.8 (0%)	13.6 (-1%)
	PAN (ppb)	14.3 (+4%)	13.6 (-1%)	13 (-6%)
	$\text{PM}_{2.5} \text{NO}_3^-$ ( $\mu\text{g m}^{-3}$ )	87 (-10%)	87 (-10%)	89 (-8%)
	$\text{PM}_{2.5}$ mass ( $\mu\text{g m}^{-3}$ )	133 (-9%)	134 (-9%)	137 (-7%)
50%	$\text{O}_3$ (ppb)	168 (-6%)	150 (-17%)	135 (-25%)
	$\text{HNO}_3$ (ppb)	11.5 (-17%)	8 (-42%)	8.5 (-39%)
	PAN (ppb)	14.4 (+5%)	8.6 (-37%)	6.2 (-55%)
	$\text{PM}_{2.5} \text{NO}_3^-$ ( $\mu\text{g m}^{-3}$ )	76 (-21%)	69 (-29%)	71 (-27%)
	$\text{PM}_{2.5}$ mass ( $\mu\text{g m}^{-3}$ )	120 (-18%)	133 (-9%)	124 (-15%)

\*These entries are the model-simulated values at Riverside, California, on 28 August 1987 for the base-case emissions inventory. Correspondence between the simulated and measured values of  $\text{O}_3$  and  $\text{PM}_{2.5} \text{NO}_3^-$  is shown in Fig. 3. The maximum 1-hour average  $\text{HNO}_3$  (13.8 parts per billion) occurred at noon. Measurements were reported as 4-hour averages; from noon to 4 p.m. the observed 4-hour average  $\text{HNO}_3$  was 5.4 ppb, as compared with the predicted 4-hour average of 6.5 ppb. Maximum total measured  $\text{PM}_{2.5}$  mass (4-hour average) was 120  $\mu\text{g m}^{-3}$ , as compared with the maximum 1-hour average prediction of 146  $\mu\text{g m}^{-3}$ .

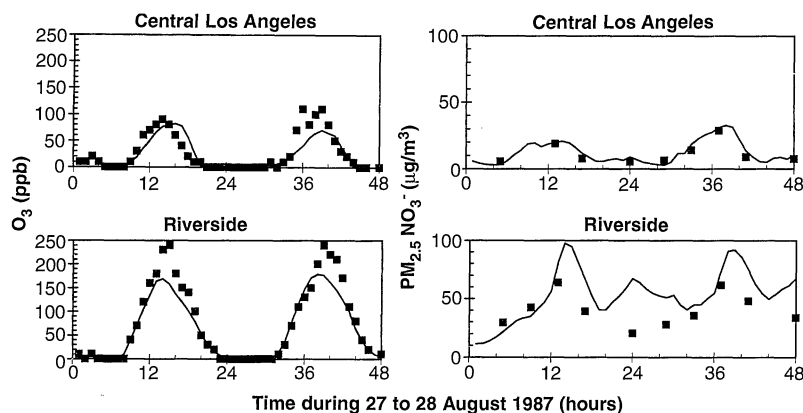


**Fig. 3.** Observed (data points) and predicted (solid line) concentrations of  $\text{O}_3$  and  $\text{PM}_{2.5} \text{NO}_3^-$  at downtown (central) Los Angeles and Riverside, California, on 27 to 28 August 1987.

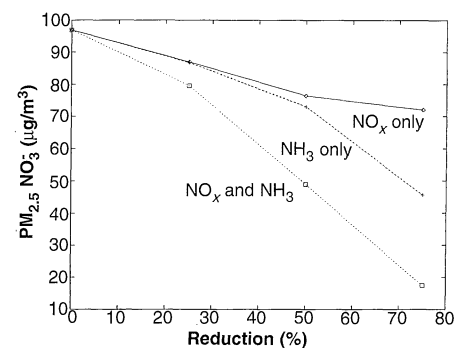


**Fig. 4.** Peak 1-hour average  $\text{PM}_{2.5}$  nitrate levels achieved at Riverside, California, on 28 August 1987 as dependent on the degree of emissions reduction from the base conditions of the episode.

imum model-predicted levels of  $O_3$ ,  $HNO_3$ , PAN, total  $PM_{2.5}$  mass, and  $PM_{2.5}$  nitrate mass at Riverside, California, on 28 August 1987. In these simulations, reductions in  $NH_3$  base emissions were not considered. Reduction in  $NO_x$  emissions alone is predicted to lead to a slight decrease in peak 1-hour average  $O_3$  levels. This behavior is consistent with the Basin being in an overall  $NO_x$ -rich state. Reductions in VOC emissions alone lead to more significant decreases in maximum  $O_3$  levels than equivalent reductions in  $NO_x$ .

An important feature of the predicted response to VOC and  $NO_x$  reductions is the behavior of  $HNO_3$ , PAN, and  $PM_{2.5}$  nitrate as either  $NO_x$  or VOC emissions are reduced. A 25% reduction in  $NO_x$  emissions at the base VOC level is predicted to lead to only a 3% reduction in peak  $HNO_3$ , a 4% increase in maximum PAN, and a 10% reduction in peak  $PM_{2.5}$  nitrate; a 50% reduction in  $NO_x$  leads to a 5% increase in PAN and a 21% reduction in maximum  $PM_{2.5}$  nitrate. When total  $NO_x$  is reduced, less  $NO_2$  is available to produce either  $HNO_3$  or PAN (reactions 1 and 3). If OH and  $RCO_3$  radical levels remain unchanged as  $NO_x$  is decreased, reactions 1 and 3 predict that both  $HNO_3$  and PAN should decrease accordingly. However, because  $HNO_3$  decreases less than proportionately and PAN actually increases, decreases of  $NO_x$  lead to increases in both OH and  $RCO_3$  levels, a behavior that is consistent with the region being in an  $NO_x$ -rich condition. If  $RCO_3$  increases considerably more than OH, then PAN levels increase while  $HNO_3$  levels exhibit a modest decrease, but one that is proportionately less than the  $NO_x$  reduction. As VOC levels are decreased, at any given  $NO_x$  level, PAN concentrations decrease as a result of the diminished availability of  $RCO_3$  radicals. As less  $RCO_3$  is available to convert  $NO_2$  to PAN, more  $NO_2$  is available to react with OH to form  $HNO_3$

(though overall OH levels are less than in the base case). Because of this increase in  $HNO_3$ ,  $PM_{2.5}$  nitrate also increases. When production of  $RCO_3$  cannot compensate for the  $NO_x$  reduction, PAN decreases also [compare PAN levels at each of 25 and 50% VOC control at 25 and 50%  $NO_x$  control (Table 1)]. Whereas our calculations are specific to the South Coast Air Basin of California, these conclusions can be expected to hold generally for any region having similar relative VOC/ $NO_x$  levels.

Maximum 1-hour  $PM_{2.5}$  nitrate levels at Riverside for emission reductions of  $NO_x$  only,  $NH_3$  only, and  $NO_x$  and  $NH_3$  together (Fig. 4) illustrate the response of particulate nitrate levels to  $NH_3$  emissions changes, which is indicative of the extent to which  $NH_3$  controls the fixation of  $HNO_3$  vapor to  $NH_4NO_3$ . For reductions of up to 50%,  $PM_{2.5}$  nitrate reductions are essentially the same for individual reductions in  $NO_x$  or  $NH_3$ ; at the 75% control level, formation becomes somewhat more  $NH_3$  controlled. That  $PM_{2.5}$  nitrate levels are substantially decreased when  $NO_x$  and  $NH_3$  are jointly reduced indicates that neither  $HNO_3$  nor  $NH_3$  individually dominates nitrate formation under current conditions.

Reduction of VOC and  $NO_x$  emissions to meet the proposed new standards for  $O_3$  and PM in those areas that are in violation will require expenditures of billions of dollars. Control strategies need to account for the intricate coupling that exists between  $O_3$  and PM. The results presented here indicate that control of gas-phase VOC and  $NO_x$  precursors generally does not lead to proportionate reductions of the secondary components of ambient particulate matter.

#### REFERENCES AND NOTES

1. National Research Council, *Rethinking the Ozone Problem in Urban and Regional Air Pollution* (National Academy Press, Washington, DC, 1991).
2. J. Schwartz, D. W. Dockery, L. M. Neas, *J. Air Waste Manage. Assoc.* **46**, 927 (1996); B. Brunekreef, D. W. Dockery, M. Krzyzanowski, *Environ. Health Perspect.* **103**, 3 (1995); X. P. Xu, J. Gao, D. W. Dockery, Y. Chen, *Arch. Environ. Health* **49**, 216 (1994); D. W. Dockery and C. A. Pope, *Annu. Rev. Public Health* **15**, 107 (1994); D. W. Dockery et al., *N. Engl. J. Med.* **329**, 1753 (1993).
3. *Fed. Reg.* **61** (no. 241), 65763 (13 December 1996).
4. *EM* (Air and Waste Management Association, Pittsburgh, PA, January 1997), pp. 16–22.
5. F. M. Bowman and J. H. Seinfeld, *J. Geophys. Res.* **99**, 5309 (1994); *Atmos. Environ.* **28**, 3359 (1994).
6. W. R. Stockwell and J. G. Calvert, *Atmos. Environ.* **17**, 2231 (1983).
7. A. S. Wexler, F. W. Lurmann, J. H. Seinfeld, *ibid.* **28**, 531 (1994).
8. S. N. Pandis and J. H. Seinfeld, *J. Geophys. Res.* **94**, 1105 (1989).
9. A. W. Stelson, S. K. Friedlander, J. H. Seinfeld, *Atmos. Environ.* **13**, 369 (1979); A. S. Wexler and J. H. Seinfeld, *ibid.* **24A**, 1231 (1990); *ibid.* **26A**, 579 (1992).
10. J. R. Odum et al., *Environ. Sci. Technol.* **30**, 2580 (1996); J. R. Odum, T. P. W. Jungkamp, R. J. Griffin, R. C. Flagan, J. H. Seinfeld, *Science* **276**, 96 (1997).
11. W. R. Pierson et al., *Atmos. Environ.* **22**, 1657 (1988); A. G. Russell et al., *Environ. Sci. Technol.* **27**, 2772 (1993).
12. C. I. Davidson and Y. L. Wu, in *Acid Precipitation*, S. E. Lindberg et al., Eds. (Springer-Verlag, Berlin, 1989), vol. 3, pp. 103–216.
13. J. H. Seinfeld, *J. Air Pollut. Control Assoc.* **38**, 616 (1988).
14. The first three-dimensional, gas-aerosol, urban-scale model was that of C. Pillinis and J. H. Seinfeld [*Atmos. Environ.* **22**, 1985 (1988)]. Development of the conservation equations on which the current model is based is given in (7). A full description of the current model used in this study, together with a detailed evaluation of the model's performance in simulating the August 1987 episode considered here, will appear in (7).
15. Y. P. Kim, J. H. Seinfeld, P. Saxena, *Aerosol Sci. Technol.* **19**, 157 (1993); *ibid.*, p. 182.
16. D. R. Lawson, *J. Air Waste Manage. Assoc.* **40**, 156 (1990); J. C. Chow et al., *Environ. Monit. Assess.* **30**, 49 (1994); J. C. Chow et al., *Atmos. Environ.* **28**, 2061 (1994).
17. Z. Meng, D. Dabdub, J. H. Seinfeld, *J. Geophys. Res.*, in press.
18. R. A. Harley, A. G. Russell, G. J. McRae, G. R. Cass, J. H. Seinfeld, *Environ. Sci. Technol.* **27**, 378 (1993).
19. We would like to acknowledge support by the Electric Power Research Institute, the IBM Environmental Research Program, the U.S. Environmental Protection Agency Center on Airborne Organics, the State of California Air Resources Board, and NSF.

29 April 1997; accepted 17 June 1997

## Discover a new sequence.

Visit the SCIENCE Online Web site and you just may find the key piece of information you need for your research. The fully searchable database of research abstracts and news summaries allows you to look through current and back issues of SCIENCE on the World Wide Web. Tap into the sequence below and see SCIENCE Online for yourself.

[www.sciencemag.org](http://www.sciencemag.org)

SCIENCE